

Geology 560 Term Paper: Seismic Refraction Analysis of the Rock Canyon Fault Zone

By Christopher M. Smemoe

Introduction

Seismic reflection and refraction methods are useful for determining and mapping the structure, stratigraphy, and lithology of the subsurface. Reflection techniques are especially useful for the exploration of hydrocarbon traps, minerals, and deep subsurface investigations. However, refraction techniques continue to be used in determining shallow subsurface structure and lithology.

In this study, seismic refraction techniques were used to determine properties of the shallow subsurface along a small traverse near the base of Rock Canyon (See Figure 1 and Figure 2). This area at the base of Rock Canyon is an area known to have faults. In fact, the Rock Canyon traverse is located along the Wasatch fault zone, which extends from southern Idaho to central Utah (See Benson and Mustoe, 1991). The subsurface anomalies along this traverse made it an ideal location for studying seismic data gathering and interpretation techniques.



Figure 1: Map showing the Rock Canyon seismic refraction survey location (courtesy of Mapquest, <http://www.mapquest.com/>)



Figure 2: Close-up map showing the location of the Rock Canyon seismic refraction survey (courtesy of Mapquest, <http://www.mapquest.com/>)

Determining the subsurface geology at the base of Rock Canyon was a three-step process. First, seismic refraction data was acquired at the Rock Canyon site. Second, this data was processed using the general reciprocal method (GRM) for seismic refractions. Third, the processed data was interpreted for fault locations and shallow subsurface lithology.

Description of Acquisition

The seismic refraction data was acquired using a large hammer with a hammer plate as the source. Geophones were spaced at twenty-foot intervals along the length of the traverse. Refraction data was collected with the source at the beginning of the traverse, at the center, and at two twenty-foot offset points, as in Figure 3.

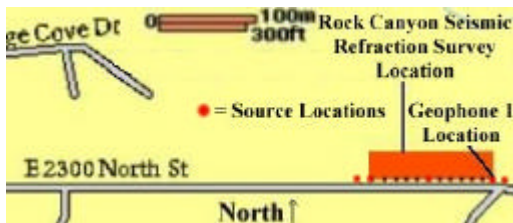


Figure 3: Rock Canyon refraction survey geophone locations (courtesy of Mapquest, <http://www.mapquest.com/>)

The tricky part of collecting data was to minimize the seismic noise at each geophone location. Cars passing by, joggers, air noise, movement in close-by houses, and other external sources caused the noise. The shot and recording was timed so these external noises would be minimized.

Data Processing

After collecting the data, the general reciprocal method (GRM) was used to process the data and determine the depth to the first contact below each geophone. To determine the depth below each geophone, the first break times were determined for each trace on each

shot seismogram. These first breaks were then plotted against the locations of the geophones, as in **Figure 4**.

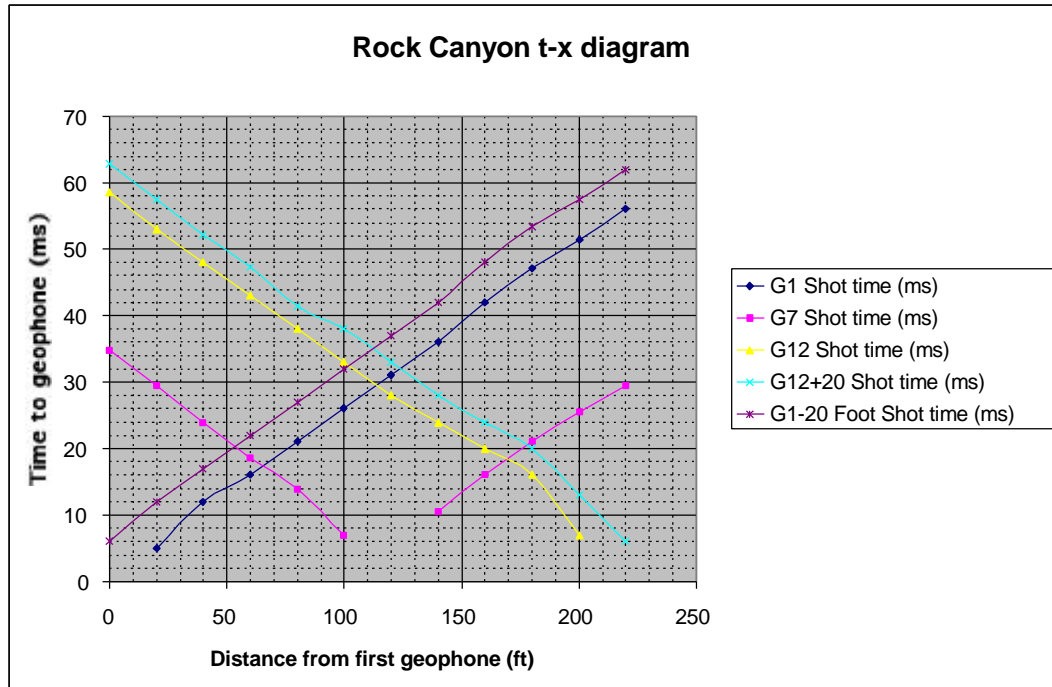


Figure 4: Rock Canyon time-distance diagram

After creating the time-distance plot in **Figure 4**, the delay time for all regions of overlapping refractors was determined according to Equation 1.

$$T_d = \frac{T_{EfG} - T_{ErG} - T_r}{2}$$

Equation 1

Where T_{EfG} is the forward first break time for a geophone, T_{ErG} is the reverse first break time for a geophone, T_r is the reciprocal time, and T_d is the delay time.

All delay times except two on each side of the time-distance diagram were determined from overlapping refractors. Additional delay times were determined by “ghosting” the first breaks of the offend shots down to the end shot. Using this method, the final four delay times at the ends (where no overlapping refractors occurred) were determined.

The velocity of the first layer was determined by averaging the forward and reverse velocities determined from the time-distance diagram. The forward velocity and reverse velocities (V_{lf} and V_{lr}) were determined from the equations below, where m is the initial slope of the line in the time-distance diagram—

$$V_{1f} = \frac{1}{m_f}, V_{1r} = \frac{1}{m_r}$$

Equation 2

The forward time minus the reverse time for regions of overlapping refractors versus the distance from the first shot point was plotted in Figure 5.

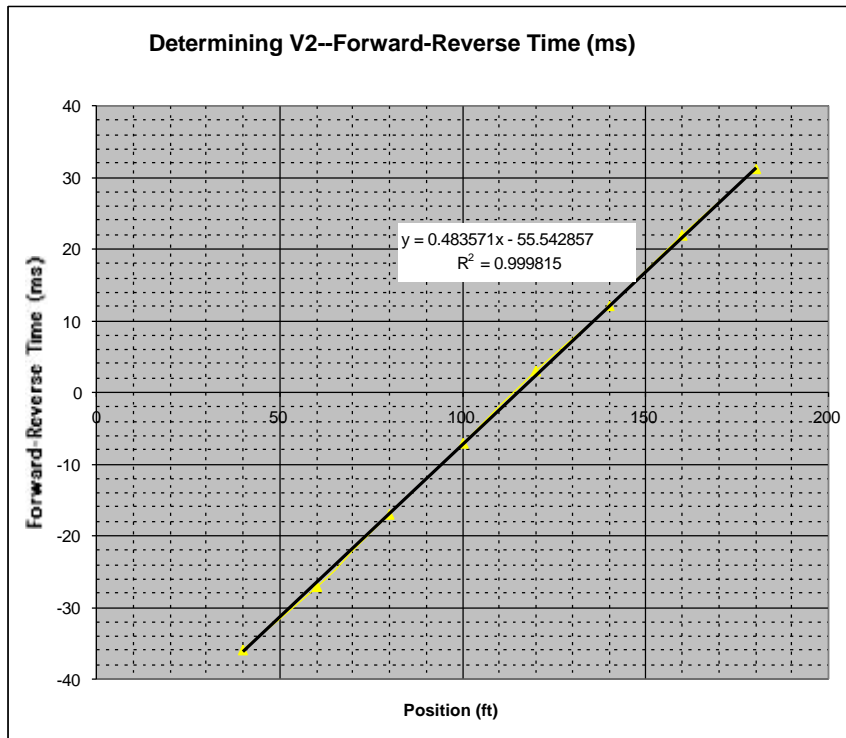


Figure 5: Plot used to determine V_2

The velocity of the second layer, V_2 , was determined from the slope of this line (m) using the equation below:

$$V_2 = \frac{2}{m}$$

Equation 3

The forward and reverse data was also modeled in the Refract Solve software to check the accuracy of the calculations in this study. The calculations were determined to be accurate, and the elevations below the first and last geophones were determined from Refract Solve. These elevations were used in the final model of the subsurface.

Finally, the depth below each geophone was determined using the delay time (T_d) and the velocities of the first and second layers (V_1 and V_2) according to the equation below:

$$z = T_d \left(\frac{V_1 \times V_2}{\sqrt{V_2^2 - V_1^2}} \right)$$

Equation 4

Data Interpretation

The ground elevation data and depth of the first refractor below each geophone were used to plot the elevation of the ground and the first refractor. After the elevations of the ground and the first refractor were determined and plotted, the plotted data was analyzed to determine the locations of faults, facies changes, and the lithology of the subsurface. The final model is shown in Figure 6.

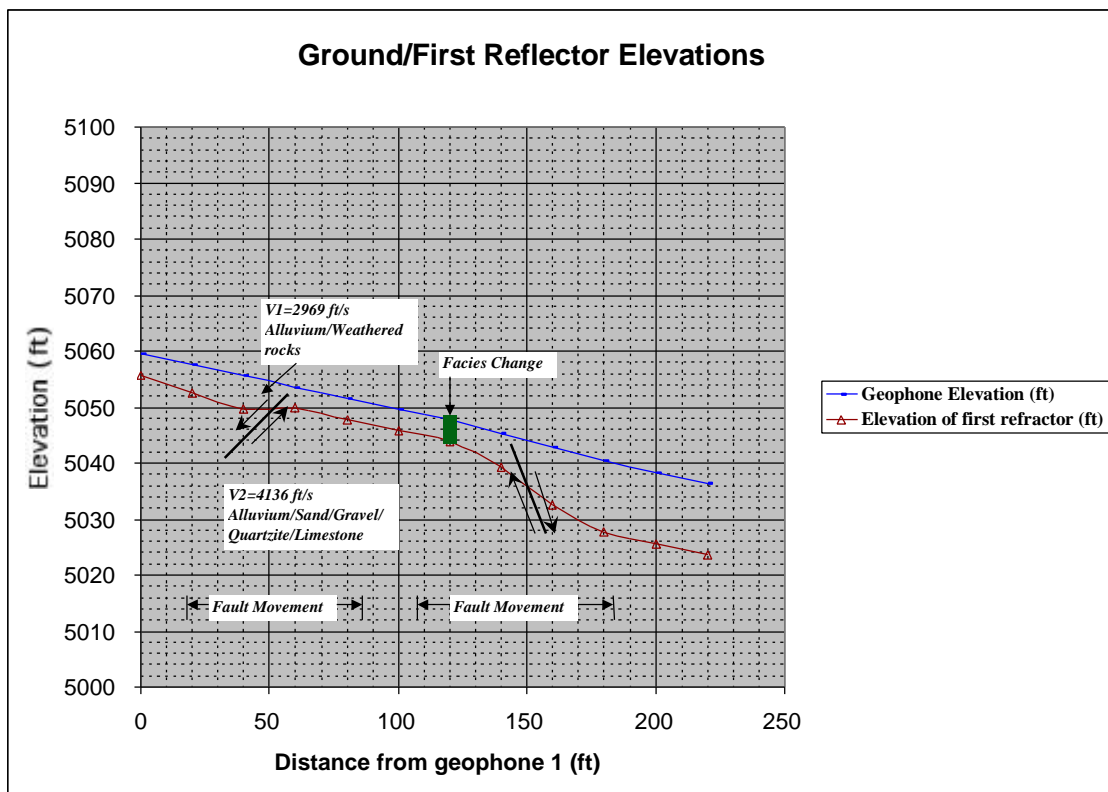


Figure 6: Geologic cross section across the refraction survey area

Figure 6 shows two positive fault locations that exist along the length of the traverse. One or more facies changes were determined to exist along the traverse since changes in first-layer velocities occurred along the traverse. The upper layer is composed of alluvium and weathered rocks, while the lower layer probably corresponds to alluvium, sand, gravel, quartzite, and/or limestone. These lithologic values were determined from the P-wave velocity table on page 18 of Burger (1992). The locations of the faults along the traverse are shown in Figure 7.

To determine the depths below the surface for the two geophone locations closest to the forward and reverse shots, the results from Refract Solve were used. The depths were also computed using the general reciprocal method, and a comparison of the results can be found in the appendix.

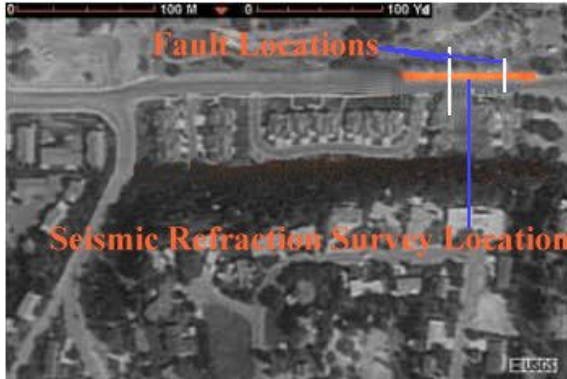


Figure 7: Aerial photo of the refraction survey area showing possible fault locations (courtesy of Microsoft Terraserver, <http://terraserver.microsoft.com/>)

Conclusion

In this study, seismic refraction data was collected, processed, and interpreted along a traverse at the mouth of Rock Canyon.

The processed seismic refraction data showed fault activity along the traverse. Lateral facies changes in the composition of the subsurface were discovered, and velocities of the first and second layers were computed.

From the seismic refraction data, it was determined that two faults existed along the seismic survey traverse. This analysis is supported by previous research, such as the research by Benson and Mustoe (1991).

References

Benson, A. K. & Mustoe, N. B. 1991. Delineating Concealed Faults and Shallow Subsurface Geology along the Wasatch Front, Utah, USA, by Integrating Geophysical and Trench Data: *Quarterly Journal of Engineering Geology*, **24**, 375-387.

Benson, A. K. & Mustoe, N. B. 1995. Analyzing Shallow Faulting at a Site in the Wasatch Fault Zone, Utah, USA, by Integrating Seismic, Gravity, Magnetic, and Trench Data: *Engineering Geology*, **40**, 139-156.

Burger, H. R. 1992. *Exploration Geophysics of the Shallow Subsurface*: Prentice-Hall, Inc., Englewood Cliffs, New Jersey, 331-335, 374-375.

Appendix: Calculations and Models